

Object Detection in Low Illumination Environment

Suk-Ho Lee
Univ. Dongseo, Korea
petrasuk@gmail.com

Seung Il Han
Univ. Dongseo, Korea
ted4sim2@naver.com

Moon Gi Kang
Univ. Yonsei, Korea
mkang@yonsei.ac.kr

ABSTRACT

We propose a motion detection algorithm which works well in low illumination environments. By using the level set based bimodal motion segmentation, the algorithm obtains an automatic segmentation of the motion region and the spurious regions due to the large CCD noise in low illumination environment are removed effectively. Based on a noise analysis, we will show how to obtain the required parameters automatically. Experimental results verify the stableness of the proposed algorithm in low illumination conditions.

Keywords: Level set, motion detection, low illumination, surveillance system.

1 INTRODUCTION

Motion detection in low illuminance environment is one of the most difficult and important problems in surveillance camera applications. Conventionally, motion detection is performed by using thresholding based methods [7][8][9][10][11] or statistical methods such as Pfunder [12], W^4 [13], Mixture of Gaussians method [14], and so on. Such methods all use some kind of a threshold value that has to be determined a priori.

However, motion detection in low illumination environment are difficult due to the following facts: First, the difficulty of setting an a priori known threshold value for segmentation[7] increases in low illumination environment, since the range of the brightness value in the difference map is narrower than in day light environment. Second, the CCD noise, which becomes more dominant when the light intensity(or the SNR) is low, causes several spurious regions that can raise the false alarm rate in intelligent surveillance camera systems.

In this paper, we propose an algorithm that deals with these problems effectively. The algorithm performs a real-time motion detection in low illumination environment as well as in day light environment, without the need of setting a threshold value and with the capability of removing spurious regions caused by the noise.

The algorithm is based on two separate level set based bimodal segmentation algorithms [4]-[6], which process a level set function such that the processed level set function classifies the image frame into the motion and the non-motion regions. The first bimodal segmentation processes the level set function such that the

level set function automatically sets the threshold value, and performs a pre-segmentation of the motion region, which contains also spurious regions. After that, a new difference map is formed using the geometric information of the pre-processed level set function, and the second bimodal segmentation processes this new difference map such that spurious regions caused by the CCD noise become entirely removed.

2 LEVEL SET BASED OBJECT DETECTION

In [4], we have proposed a model that implements a bimodal segmentation based on the competition of the brightness values in an image. The segmented regions are represented via a level set function ϕ which minimizes the following energy functional:

$$E(\phi) = \lambda_1 \int_{\Omega} |u_0(\mathbf{r}) - \text{ave}_{\{\phi \geq 0\}}|^2 \phi(\mathbf{r}) H(\alpha + \phi(\mathbf{r})) d\mathbf{r} \\ - \lambda_2 \int_{\Omega} |u_0(\mathbf{r}) - \text{ave}_{\{\phi < 0\}}|^2 \phi(\mathbf{r}) H(\alpha - \phi(\mathbf{r})) d\mathbf{r} \quad (1)$$

where λ_1, λ_2 are non-negative parameters, α is an arbitrary small positive value, $u_0(\mathbf{r})$ is the given image, Ω is the domain of the given image u_0 , ϕ is the level set function, and $\text{ave}_{\{\phi \geq 0\}}, \text{ave}_{\{\phi < 0\}}$ are the average values of $u_0(\mathbf{r})$ in the 2-D regions $\{\phi \geq 0\}$ and $\{\phi < 0\}$, respectively. Here, $H(\phi)$ is the one-dimensional Heaviside function with $H(s) = 1$ if $s \geq 0$, and $H(s) = 0$ if $s < 0$. In [4], the following theorem was proved.

Theorem 2.1 Assume u_0 is a continuous function. Let, $\Lambda_{\phi}(\mathbf{r}) := |u_0(\mathbf{r}) - \text{ave}_{\{\phi \geq 0\}}|^2 - |u_0(\mathbf{r}) - \text{ave}_{\{\phi < 0\}}|^2$ and

$$\text{sign}(\Lambda_{\phi}(\mathbf{r})) := \begin{cases} 1 & \text{if } \Lambda_{\phi}(\mathbf{r}) > 0 \\ -1 & \text{if } \Lambda_{\phi}(\mathbf{r}) < 0 \\ 0 & \text{if } \Lambda_{\phi}(\mathbf{r}) = 0. \end{cases}$$

Then, if $\phi(\mathbf{r})$ is a minimizer for the energy functional $E(\phi)$ in (1), $\text{sign}(\Lambda_{\phi}(\mathbf{r}))\phi(\mathbf{r}) = -\alpha$, i.e., $\phi(\mathbf{r}) = -\text{sign}(\Lambda_{\phi}(\mathbf{r}))\alpha$, whenever $\text{sign}(\Lambda_{\phi}(\mathbf{r})) \neq 0$.

Permission to make digital or hard copies of all or part of this work for personal or classroom use is granted without fee provided that copies are not made or distributed for profit or commercial advantage and that copies bear this notice and the full citation on the first page. To copy otherwise, or republish, to post on servers or to redistribute to lists, requires prior specific permission and/or a fee.

The theory states that the energy of the energy functional in (1) is minimized when every \mathbf{r} at which $|u_0(\mathbf{r}) - ave_{\{\phi \geq 0\}}|^2 < |u_0(\mathbf{r}) - ave_{\{\phi < 0\}}|^2$ is classified in the region $\{\mathbf{r} \mid \phi(\mathbf{r}) = -\alpha\}$, and every \mathbf{r} at which $|u_0(\mathbf{r}) - ave_{\{\phi \geq 0\}}|^2 > |u_0(\mathbf{r}) - ave_{\{\phi < 0\}}|^2$ is classified in the region $\{\mathbf{r} \mid \phi(\mathbf{r}) = \alpha\}$ with an arbitrary initial level set function. In the steady state, the ϕ function becomes a piecewise continuous function having either the value α or $-\alpha$ at each point, and the zero level set of ϕ becomes the contour that segments the image region into two regions based on the competition of the colors. Since the segmentation result depends on the competition of the colors, that is, on the relative relationship of the colors, the segmentation result is adaptive to the image.

The adaptive property of the bimodal segmentation makes it useful for motion detection. As mentioned in the introduction, the object is normally segmented by segmenting the background subtracted frame, where the threshold value varies from scene to scene. However, the bimodal segmentation algorithm segments the object without thresholding, and therefore the segmentation process becomes adaptive to the image and automatical, since there is no need to set an a priori known threshold value. In the bimodal segmentation scheme, we use instead of u_0 in (1), the background subtracted frame $\mathbb{D}u$.

When the SNR of the image becomes very low, then the noise becomes apparent in the difference frame, and some pixels, at which the intensity difference value exceeds the average intensity difference between the two regions, become classified in the counterpart region. Figure 1(a)-(c) shows the background frame, the current frame, and the difference frame of a scene obtained in the night. Figure 1(d) shows the segmentation result with the bimodal segmentation. Even though the bimodal segmentation segments the regions automatically, due to the noise, there appears many spurious regions in the segmented regions.

Figure 1(d) shows that the ϕ function has several outliers(dotted points), which result in falsely segmented regions. Hereafter, we refer to the noise as the outliers in the ϕ function, that is, the points which have falsely converged to α (or $-\alpha$), instead of $-\alpha$ (or α). To eliminate such outliers, certain regularization terms which suppress spatial discontinuity in the ϕ function have to be used together with the bimodal term.

3 LEVEL SET BASED MOTION DETECTION WITH HARMONIC REGULARIZATION

Various energy functionals that use the magnitude of the gradient of the image can be used as the regularization term to suppress the noise. A well-known regularization term is the total variation regularization

term. Using this term together, the energy functional becomes:

$$\begin{aligned} E(\phi) = & \lambda_1 \int_{\Omega} |\mathbb{D}u(\mathbf{r}) - ave_{\{\phi \geq 0\}}|^2 \phi(\mathbf{r}) H(\alpha + \phi(\mathbf{r})) d\mathbf{r} \\ & - \lambda_2 \int_{\Omega} |\mathbb{D}u(\mathbf{r}) - ave_{\{\phi < 0\}}|^2 \phi(\mathbf{r}) H(\alpha - \phi(\mathbf{r})) d\mathbf{r} \\ & + \beta \int_{\Omega} |\nabla \phi| d\mathbf{r}, \end{aligned} \quad (2)$$

where we denoted by $\mathbb{D}u$, the background subtracted frame, and where α and β are an arbitrary positive value, and Ω is the domain of the given image $\mathbb{D}u$.

The corresponding gradient descent flow equation with respect to ϕ is :

$$\begin{aligned} \phi_t = & \beta \nabla \cdot \left(\frac{\nabla \phi}{|\nabla \phi|} \right) \\ & - \lambda_1 |\mathbb{D}u(\mathbf{r}) - ave_{\{\phi \geq 0\}}|^2 \{H(\alpha + \phi(\mathbf{r})) + \phi H'(\alpha + \phi(\mathbf{r}))\} \\ & + \lambda_2 |\mathbb{D}u(\mathbf{r}) - ave_{\{\phi < 0\}}|^2 \{H(\alpha - \phi(\mathbf{r})) - \phi H'(\alpha - \phi(\mathbf{r}))\}. \end{aligned}$$

However, a faster algorithm than using the total variation term as the regularization term is the one with harmonic regularization. The harmonic regularization uses the L_2 norm of the magnitude of the gradient of the image and thus the smoothing speed is faster than the total variation regularization. The bimodal segmentation with harmonic regularization has the following energy functional form:

$$\begin{aligned} E(\phi) = & \lambda_1 \int_{\Omega} |\mathbb{D}u(\mathbf{r}) - ave_{\{\phi \geq 0\}}|^2 \phi(\mathbf{r}) H(\alpha + \phi(\mathbf{r})) d\mathbf{r} \\ & - \lambda_2 \int_{\Omega} |\mathbb{D}u(\mathbf{r}) - ave_{\{\phi < 0\}}|^2 \phi(\mathbf{r}) H(\alpha - \phi(\mathbf{r})) d\mathbf{r} \\ & + \beta \int_{\Omega} |\nabla \phi|^2 d\mathbf{r}, \end{aligned} \quad (3)$$

Here, the choice of β will depend on the noise structure of the difference image.

The corresponding gradient descent flow equation with respect to ϕ is :

$$\begin{aligned} \phi_t = & \beta \nabla^2 \phi \\ & - \lambda_1 |\mathbb{D}u(\mathbf{r}) - ave_{\{\phi \geq 0\}}|^2 \{H(\alpha + \phi(\mathbf{r})) + \phi H'(\alpha + \phi(\mathbf{r}))\} \\ & + \lambda_2 |\mathbb{D}u(\mathbf{r}) - ave_{\{\phi < 0\}}|^2 \{H(\alpha - \phi(\mathbf{r})) - \phi H'(\alpha - \phi(\mathbf{r}))\}. \end{aligned}$$

Normally, in image denoising, it is preferred to use the total variation regularization term, since it preserves edges, and the intensity value of large scale structures varies not much. However, in smoothing the ϕ function, the change in the magnitude of the ϕ value is not of interest as long as it does not change its sign, since it is the sign of the $\phi(\mathbf{r})$ value and not the magnitude value that determines the classification. Sharp edges in the ϕ function become smeared by the harmonic regularization term, but the smearing is not so critical an artifact as in image denoising, since the position of



Figure 1: Showing the result of object detection with level set based bimodal segmentation without using regularization terms. (a) current frame (b) background frame (c) absolute difference frame (d) segmentation result (level set function).

the zero level set will not change much by the smearing process. Therefore, the harmonic regularization term can achieve similar classification result as the total variation regularization term, while being faster. Since, in video processing the speed is the more important factor we prefer (3) to (2).

Clearly, the regularization process should have a larger effect if the SNR becomes lower. Therefore, the parameter β is dependent on the SNR. Therefore, we give here a rough analysis on the relationship between the parameter β and the noise, and show how to choose the parameter β .

We denote by $\Psi[\phi](\mathbf{r})$ the integrand of the energy functional in (1):

$$\Psi[\phi](\mathbf{r}) := + |u_0(\mathbf{r}) - ave_{\{\phi \geq 0\}}|^2 \phi(\mathbf{r}) H(\alpha + \phi) - |u_0(\mathbf{r}) - ave_{\{\phi < 0\}}|^2 \phi(\mathbf{r}) H(\alpha - \phi), \quad (4)$$

As stated in theorem 2.1, in the steady state this integrand converges to α or to $-\alpha$ according to the intensity value at the pixel corresponding to the integrand. Now, together with the harmonic regularization term, the new integrand becomes,

$$\Psi[\phi](\mathbf{r}) := + |u_0(\mathbf{r}) - ave_{\{\phi \geq 0\}}|^2 \phi(\mathbf{r}) H(\alpha + \phi) - |u_0(\mathbf{r}) - ave_{\{\phi < 0\}}|^2 \phi(\mathbf{r}) H(\alpha - \phi) + \beta |\nabla \phi|^2 \quad (5)$$

We will compute the minimum value of this integrand for a “one-pixel noise” model. In the “one-pixel noise” model it is assumed that there is no other noisy pixel in the neighborhood of the noisy pixel. Figure 4 shows this “one-pixel noise” model for the one-dimensional case. Here, the values $\phi_a = -\alpha, \phi_b = \alpha$, and $\phi_c = -\alpha$ are assumed to be the ϕ values at the steady state of (2) without the harmonic regularization term, where pixel ‘b’ corresponds to the noisy pixel, and ‘a’ and ‘c’ are the rightly classified pixels. By denoising, we mean that the ϕ value of ‘b’ drops below zero, so that sign of the ϕ values of ‘a’, ‘b’, and ‘c’ all become the same, i.e., negative.

First, we compute the minimizer ϕ value of ‘b’ with the harmonic regularization, i.e., the minimizer of (5), with β fixed. Then, we find the condition of β which makes the ϕ value of ‘b’ negative. Definitely, the minimizer at which the energy of the integrand reaches the minimum cannot be outside the interval $|\phi| < \alpha$, since

this would make both the energy of the bimodal term and the harmonic regularization term increase. Therefore, the minimizer must lie in the interval $|\phi| < \alpha$, which is the point ϕ'_b in Fig. 4. In this interval the two Heaviside functions in (5) become both 1, and the integrand becomes

$$\Psi[\phi](\mathbf{r}) := \Lambda(u_0, \phi) \phi(\mathbf{r}) + \beta |\nabla \phi|^2, \quad (6)$$

where $\Lambda(u_0, \phi) = \left[|u_0(\mathbf{r}) - ave_{\{\phi \geq 0\}}|^2 - |u_0(\mathbf{r}) - ave_{\{\phi < 0\}}|^2 \right]$. Even though $\Lambda(u_0, \phi)$ is a function of ϕ , the one point denoising has scarcely any effect on the change of $ave_{\{\phi \geq 0\}}$ or $ave_{\{\phi < 0\}}$, therefore, to make the analysis simple, we regard $\Lambda(u_0, \phi)$ as a constant with respect to ϕ , and denote it by $\Lambda(u_0)$. We also use the discretized version of the harmonic regularization term, that is, we let

$$\begin{aligned} |\nabla \phi_{min}|^2 &= (\phi'_b - \phi'_a)^2 + (\phi'_b - \phi'_c)^2 \\ &= 2(\phi'_b - \phi'_a)^2 \\ &= 2(x - (-\alpha + \frac{x}{2}))^2 = 2(\alpha - \frac{x}{2})^2 \end{aligned} \quad (7)$$

where ϕ_{min} is the minimum ϕ value of (6). Here, x is the solution we are looking for. We assumed that the change in magnitude of the ϕ value of point ‘a’ is twice those of point ‘b’ and ‘c’. This assumption is supported by the fact that the noisy pixel ‘a’ has on both sides ϕ values that differ by 2α , whereas the pixels ‘b’ and ‘c’ have it only on one side. With this assumption, the ϕ value which makes the integrand in (6) smallest becomes

$$\phi_{min}(\mathbf{r}) = - \left(\alpha + \frac{\Lambda(u_0)}{4\beta} \right). \quad (8)$$

In our one-pixel noise example, denoising means that the sign of the current ϕ value has changed from a positive value to negative value. The condition for $\phi_{min}(\mathbf{r})$ to become a negative value is,

$$\begin{aligned} \phi_{min}(\mathbf{r}) &= - \left(\alpha + \frac{\Lambda(u_0)}{4\beta} \right) < 0 \\ \Leftrightarrow \beta &> - \frac{\Lambda(u_0)}{4\alpha} \end{aligned} \quad (9)$$

where it has to be kept in mind that $\Lambda(u_0)$ is negative in our example. The value of $\Lambda(u_0)$ is related to the amount of the noise in the image. It can be seen from (9) that if the noise becomes larger than β has to be larger to eliminate the noise. Intuitively, we see that

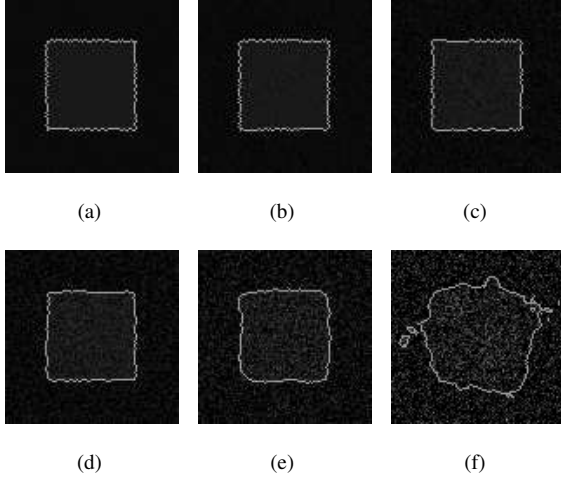


Figure 2: Result of automatically setting the β value, and applying the harmonic regularized bimodal segmentation on simulated images. (a) SNR =30 (b) SNR =25 (c) SNR = 20 (d) SNR = 15 (e) SNR = 10 (f) SNR = 5

$\Lambda(u_0)$ is somehow proportionally related to the variance of the noise. Therefore, after estimating the variance of the noise through some existing estimating method, we set the value of β to

$$\beta = 3 \left(\frac{Var_{noise}}{4\alpha} \right). \quad (10)$$

Figure 2 shows the result of setting the β value as in (10) and then performing the harmonic regularized bimodal segmentation on simulated images with different SNR values. The intensity difference of the box in the middle and the outside is 8. It can be seen that the automatic setting of the β value results in good results when the SNR is large. However, as the SNR value decreases, the shape of the zero level set distorts much. Therefore, in the next section, we propose a method for eliminating the spurious regions due to the noise.

4 LEVEL SET BASED MOTION DETECTION WITH ELIMINATION OF SPURIOUS REGIONS

For a further elimination of spurious regions due to the noise, we can take extra elimination steps. These extra steps can also be directly applied on the level set function obtained by the bimodal segmentation without regularization term, to give good elimination results. The elimination of spurious regions is performed in the following three steps: First, calculate a mean curvature map from the processed level set function obtained by (3). Second, calculate a new difference map by normalizing the original difference map with respect to the mean curvature map, and taking the segmentation result in section 2 into account. Third, perform a regularized

bimodal segmentation on the new difference map.

To calculate the mean curvature map, the level set function obtained from (3) is first binarized, where the binarized pixel values corresponding to the region $\{\mathbf{r}|\phi(\mathbf{r}) \geq 0\}$ are 1, and those corresponding to the region $\{\mathbf{r}|\phi(\mathbf{r}) < 0\}$ are 0. Then, regarding the binarized image as a two dimensional surface in the three dimensional space, with the binarized pixel value corresponding to the z axis, the mean curvature is computed at each pixel. The mean curvature value can be regarded as a measure that measures the amount by which the image structures deviate from being flat. As a result, small image structures like spurious regions due to the noise tend to have large mean curvature values. Therefore, if the region in the difference map corresponding to the motion region obtained by (3) is divided by the mean curvature map, then most of the spurious regions will have relatively small values in the new difference map. The new difference map is obtained by dividing the original difference map ($\mathbb{D}I$) by the mean curvature map \mathbb{M} and normalizing it as follows:

$$\mathbb{D}I_{new}(\mathbf{r}) = \begin{cases} \frac{\mathbb{D}I(\mathbf{r})}{\mathbb{M}(\mathbf{r}) \mathbb{D}I_{max}}, & \text{if } \phi(\mathbf{r}) \geq 0 \\ 0, & \text{if } \phi(\mathbf{r}) < 0 \text{ or } \mathbb{M}(\mathbf{r}) = 0, \end{cases} \quad (11)$$

where ϕ is the level set function obtained by (3), $\mathbb{M}(\mathbf{r})$ is the mean curvature value at the position \mathbf{r} , and $\mathbb{D}I_{max}$ is the maximum of all the $\mathbb{D}I_{new}(\mathbf{r})$ values.

Figure 5(h) shows the mean curvature map calculated from the binarized level set function, and Fig. 5(i) shows the corresponding normalized new difference map. The effect of dividing by the curvature map can be seen by comparing Fig. 5(f) and Fig. 5(i). The dense noise with relatively large intensity values in Fig. 5(f) appear to have become sparse in the new difference map, since small image structures have experienced a large decrease in their intensity values by the division through the mean curvature value. Therefore, if now a level set based bimodal segmentation with harmonic regularization is performed on the new difference map, the spurious regions due to the noise become entirely eliminated by the harmonic regularization.

The level set based bimodal segmentation with harmonic regularization term solves the following differential equation:

$$\frac{d\hat{\phi}}{dt} = \frac{1}{c_1 + c_2} (\mathbb{D}I_{new} - c_2)^2 - \frac{1}{c_1 + c_2} (\mathbb{D}I_{new} - c_1)^2 + \nabla^2 \hat{\phi} \quad (12)$$

The equation is the same as (3), except for the harmonic regularization term ($\nabla^2 \hat{\phi}$). The first and the second term in the righthand side are normalized with respect to $c_1 + c_2$ such that the harmonic regularization term can compete with these terms. The harmonic regularization term smooths out the level set function fast such that the sparse spurious regions due to the sparse noise

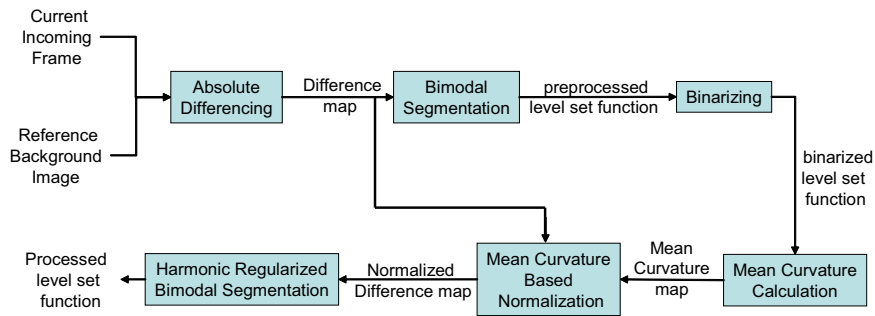


Figure 3: Overall block diagram of proposed method.

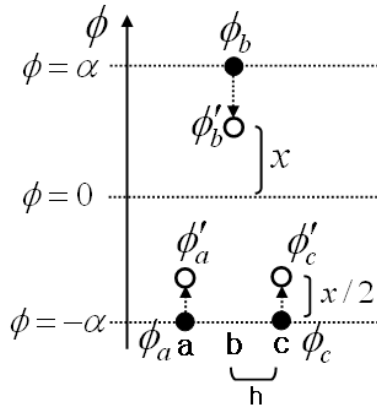


Figure 4: One-pixel noise model in 1-D

in the new difference map become entirely eliminated, while the valid motion regions survive due to the strong influence of the first two fidelity terms.

The segmentation result that results from the competition can be seen in Fig. 5(f), which shows the motion region represented by the region $\{\mathbf{r} \mid \hat{\phi}(\mathbf{r}) \geq 0\}$. The spurious regions have been effectively eliminated while motion regions are well preserved. For comparison, Fig. 5(g) illustrates how a simple application of a morphological filter can fail in the complete elimination of spurious regions. Figure 5(d) shows the result of using a threshold based method and Fig. 5(e) shows the result of the MOG (Mixture of Gaussian) method with threshold value 0.7 to segment the object. It can be seen that the a priori given threshold value can result in a loss of the object region or produce spurious regions. Figure 3 shows the overall block diagram of the proposed motion detection method. Figure 6 shows the object detection result of the proposed method. The proposed method works in real time on a 320×240 frame with 2.1GHz PC due to the fast bimodal segmentation algorithm, which takes just 3–5 iterations for the classification.

5 CONCLUSION

In this paper, we presented a motion detection scheme that sets its target especially for motion detection in low illuminance environment. It is shown that the proposed

scheme can detect moving objects well even in very low illumination conditions and without the need of setting an a priori known threshold value and with the capability of eliminating spurious regions.

6 ACKNOWLEDGEMENT

This work was supported by the Korea Research Foundation Grant funded by the Korean Government (MOEHRD, Basic Research Promotion Fund) (KRF-2008-331-D00566).

REFERENCES

- [1] P.L. Rosin and T. Ellis. "Image difference threshold strategies and shadow detection," In Proceedings of the 6th British Machine Vision Conference, pp. 347–356, BMVA Press, 1995.
- [2] Osher, S. and Fedkiw, R., "Level Set Methods and Dynamic Implicit Surfaces," Springer-Verlag, New York, (2002).
- [3] Sethian, J.A., "Level Set Methods and Fast Marching Methods," Second Edition, Cambridge University Press, Cambridge, UK, 1999.
- [4] S.H. Lee and J.K. Seo, "Level Set-Based Bimodal Segmentation With Stationary Global Minimum," IEEE Trans. on Image Processing, vol. 15, no. 9, pp. 2843–2852, Sep. 2006.
- [5] Gibou, F. and Fedkiw, R., "A Fast Hybrid k-Means Level Set Algorithm for Segmentation," 4th Annual Hawaii International Conference on Statistics and Mathematics, pp. 281–291, Stanford Technical Report, Nov. 2002.
- [6] T.F. Chan and L.A. Vese, "Active contours without edges," IEEE Trans. on Image Processing, vol. 10, no. 2, pp. 266–277, Feb. 2001.
- [7] P.L. Rosin and T. Ellis. "Image difference threshold strategies and shadow detection," In Proceedings of the 6th British Machine Vision Conference, pp. 347–356, BMVA Press, 1995.
- [8] G. Halevy and D. Weinshall, "Motion of disturbances: detection and tracking of multibody non-rigid motion", Machine Vision and Applications, vol. 11, pp. 122-137, 1999.

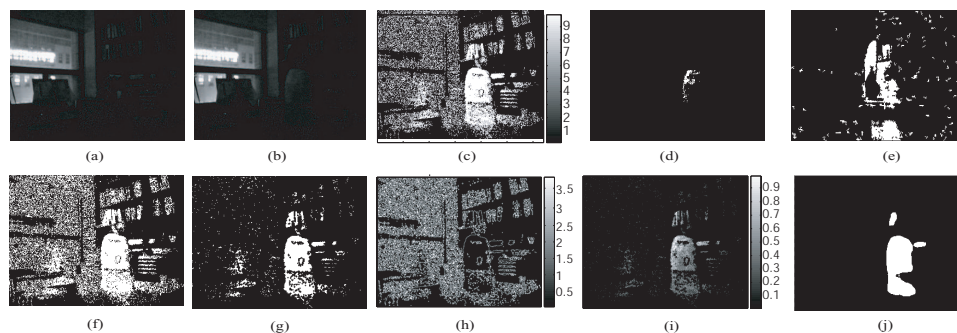


Figure 5: Segmentation result in low illumination environment: (a) reference background frame, (b) incoming current frame, (c) difference map, (d) result of thresholding the difference map (c) with threshold value=20, (e) result of MOG method (f) segmentation result using (3) in section 2, (g) result of eroding the image in (f) with morphological filter, (h) mean curvature map, (i) new difference map, (j) final segmentation result with proposed method.

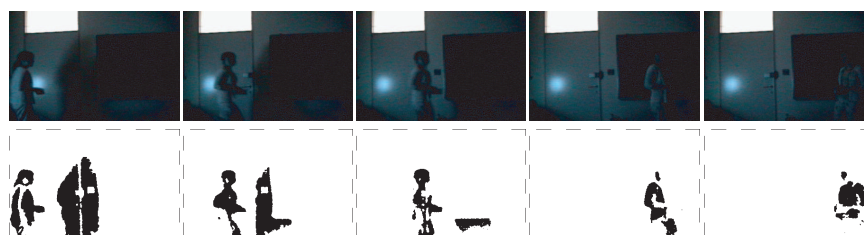


Figure 6: Object detection result with the proposed method.

- [9] J. Heikkila and O. Silven, "A real-time system for monitoring of cyclists and pedestrians," Second IEEE Workshop on Visual Surveillance, pp. 74-81, July 1999.
- [10] P. L. Rosin and E. Ioannidis, "Evaluation of global image thresholding for change detection," vol. 24, Pattern Recognition Letters, pp. 2345-2356, 2003.
- [11] E. Stringa, "Morphological change detection algorithms for surveillance applications," Proc. Brit. Machine Vision Conf., 2000.
- [12] C. Wren, A. Azarbayejani, T. Darrell, and A. Pentland, "Pfinder: Real-Time Tracking of the Human Body," IEEE Trans. on Pattern Analysis and Machine Intelligence, vol. 19, pp. 780-785, 1997.
- [13] I. Haritaoglu, D. Harwood, and L. S. Davis, "W⁴: Who? When? Where? What? a real time system for detecting and tracking people", Third International Conference on Automatic Face and Gesture Recognition, pp. 222-227, April 1998,.
- [14] C. Stauffer and W. E. L. Grimson, "Adaptive background mixture models for real-time tracking," Computer Vision and Pattern Recognition, Fort Collins, Colorado Jan pp. 246-252, 1999.